An analysis of the magnetic ground state in yttrium iron garnets

1995 J. Phys.: Condens. Matter 7 1391

(http://iopscience.iop.org/0953-8984/7/7/019)

J. Phys.: Condens. Matter 7 (1995) 1391–1404. Printed in the UK

An analysis of the magnetic ground state in yttrium iron garnets

A Koper, A Lehmann-Szweykowska, R Wojciechowski and M Mucha
Institute of Physics, A. Mickiewicz University, Poznań, Poland

Received 4 August 1994, in final form 10 November 1994

Abstract. We analyse the magnetic phase diagram of yttrium iron garnet (YIG) at $T = 0$ K (in the MFA approximation) described by a Heisenberg Hamiltonian. There are five different phases and one spin-flop line. Two of these phases are of different semi-spin-glass type. In order to adequately describe them we introduce two new notions: *the correlation density function* and *the information entropy of the correlation density functions*. The functions and their entropies are calculated by means of a Monte Carlo method. We discovered that the ferrimagnetic point of the phase diagram corresponding to real YIG falls in the area where three different phases converge. One of these phases is of semi-spin-glass type. The results obtained can shed light on the interpretation of the low-temperature properties of YIG doped with charge uncompensated ions, for example Ca^{2+}.

1. Introduction

In this paper we provide a detailed description of the ground-state phase diagram of a magnetic system with the crystalline structure of yttrium iron garnet $Y_3Fe_5O_{12}$ (YIG). The diagram was obtained by means of the so-called relaxation method [1, 2]. In the case of classical spin Hamiltonians the method gives exact numerical results. In the case of quantum systems this method is equivalent to the version of MFA, where for each lattice site the molecular field equation is solved separately.

In our calculation we assumed that the sources of localized magnetic momenta are only the trivalent iron ions Fe^{3+} ($3d^5$) which are in spin-like multiplets $^6S_0$ with no orbital contribution ($L = 0$) and an effective spin equal to $\frac{5}{2}$. The ions occupy two inequivalent magnetic sublattices: octahedral (a) and tetrahedral (d). The third sublattice, dodecahedral (c), is occupied by diamagnetic ions Y^{3+} ($4p^6$).

We also assumed that there is a superexchange coupling between Fe^{3+} ions (through the O^{2-} ($2p^6$) ions) and that we may restrict interactions to nearest neighbours. The interactions are described by the Heisenberg Hamiltonian.

There are five different phases and one spin-flop line on the obtained diagram. It is astonishing that two of these phases are of the semi-spin-glass type. We think that the occurrence of these phases is a consequence of the YIG geometry. Equally astonishing is the fact that the ferrimagnetic point G of the phase diagram (see figure 1(a)) corresponding to the real $Y_3Fe_5O_{12}$ yttrium iron garnet lies in the area where three different phases converge. One of these phases happens to be of the semi-spin-glass type. We took the location of the point G from [3]. There is no consensus as to the actual location of the point. We shall return to this problem in the final section of this paper.

The location of the point G in the diagram might explain some of the properties of the $(Y_{3-x}Ca_x)Fe_5O_{12}$ YIG doped with valence-uncompensated Ca^{2+} ions. The doped ions

0953-8984/95/071391+14$19.50

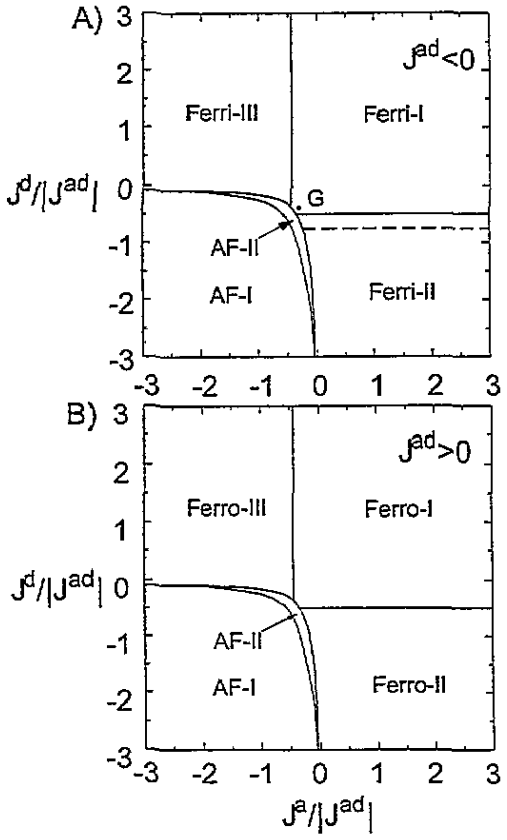

Figure 1. (*a*) Magnetic phase diagrams of the ground state for $J^{ad} < 0$. The broken line denotes the spin flop phase. G is the position corresponding to the experimentally determined values of the superexchange integrals J^a, J^d and J^{ad} for a real $Y_3Fe_5O_{12}$ garnet [3]. (*b*) Magnetic phase diagrams of the ground state for $J^{ad} > 0$.

replace Y^{3+}, which leads to a low-temperature decrease of its saturation magnetization, photoinduced susceptibility, optoelectrical and photomemory effects [4]. It is worth noting that the spin-glass phase was found experimentally [5] in mixed compounds similar to the YIG-like $(Fe_xCr_{1-x})_2Ca_3(GeO_4)_3$. In section 5 we briefly discuss the relation between the phase diagram that we obtained with the behaviour of YIG doped with Ca^{2+}. However, we think that this problem requires a more detailed analysis [6] (despite the fact that some aspects have already been presented [7, 8]) within the framework of a previously introduced model [9, 10]: an adaptation of the usual periodic Anderson model for the narrow- band (3d) and wide-band (2p) electrons with the (p–d) hybridization term.

The paper is organized as follows. In section 2 we briefly discuss a model of magnetic interactions in YIG. We elaborate on the symmetries of the quantum Heisenberg Hamiltonian, which play a crucial role in further analyses of the problem.

In section 3 we describe methods of calculation. The basic method consists in replacing the quantum Heisenberg Hamiltonian H with its classical equivalent, i.e. the Hamilton function $\mathcal{H}$. It can be shown that local minima of that function may be interpreted as metastable variational states of the Hamiltonian H, where the role of the trial state space is played by coherent spin states [11]. In section 3.1 we discuss the valley structure of the function $\mathcal{H}$ and in section 3.2 we discuss the relaxation method, which enables an exact determination of the local minima of this function. In section 3.3 we introduce the concept of the correlation function density and its informational entropy in the spin-glass phase. These newly introduced notions enable us to precisely distinguish different points in the

spin-glass phase.

In section 4 we consider our results. Section 4.1 is devoted to a discussion of the phase diagram, and section 4.2 to the density of the correlation function in the semi-spin-glass phase. Section 5 contains our conclusions, a summary of our results and their interpretation in the context of doped YIG $(Y_{3-x}Ca_x)Fe_5O_{12}$.

2. A model of magnetic interactions in yttrium iron garnet (YIG)

As is commonly known, the elementary unit cell of YIG contains 16 iron ions occupying 16 different (a) sites, and 24 iron ions occupying 24 different (d) sites. The positions of these 40 magnetic ions are gathered in [12]. The symmetry of the crystal structure of YIG is determined by the 96-element space group, O_h^{10}. Magnetic interactions in YIG can be described by the usual translationally invariant two-sublattice Heisenberg Hamiltonian:

$$\hat{H} = -\frac{1}{2}\sum_{i\neq j} J_{ij}^{a}\hat{s}_i\hat{s}_j - \frac{1}{2}\sum_{k\neq l} J_{kl}^{d}\hat{s}_k\hat{s}_l - \sum_{i,k} J_{ik}^{ad}\hat{s}_i\hat{s}_k \tag{1}$$

where $\hat{s}_i$ are the $\frac{5}{2}$ spin operators and in the last term the summation runs over sites of different sublattices; J_{ij}^{a}, J_{ij}^{d}, J_{ij}^{ad} denote, in order, the nearest-neighbour intra- and inter-sublattice superexchange integrals. The coordination numbers are equal to $\gamma_{aa} = 8$, $\gamma_{dd} = 4$, $\gamma_{ad} = 6$, $\gamma_{da} = 4$, respectively, where, for instance, γ_{ad} is the number of nearest neighbours of the site a in the sublattice (d).

The Hamiltonian (1) has several symmetries which play an important part in our interpretation of the properties of its ground energy level. The global group of the symmetry of the operator (1) is the three-dimensional matrix group $O(3)$ of the spins. This explains why all the eigenvalues of the Hamiltonian (1) have a trivial infinite degeneracy of the order of the continuum. The group $O(3)$ is the gauge group of the problem. Consequently, the degeneracy of the ground energy level which does not result from the group $O(3)$ will be considered non-trivial.

As well as the space symmetry group O_h^{10}, which has been already mentioned, another discrete group of transformations is associated with the Hamiltonian (1):

$$\mathcal{G} = \{e, \tau_a, \tau_d, \tau\} \tag{2}$$

where e is the unit operator, and τ is the operator of inversion, i.e. $\tau\hat{s}_i = -\hat{s}_i$ $(i \in a, d)$. The operator τ_a acts only on the spins of the sublattice (a) i.e. $\tau_a\hat{s}_i = -\hat{s}_i$ if $i \in a$. Analogously, the operator τ_d changes orientations of spins of the sublattice (d). We shall call the group $\mathcal{G}$ the inversion group. As will be shown later the group $\mathcal{G}$ essentially affects the global form of magnetic phase diagrams.

Let $\hat{S}_a$ and $\hat{S}_d$ denote all the spins of the sublattices (a) and (d), respectively. It is then easy to notice that

$$\hat{H}(\hat{S}_a, \hat{S}_d, J^a, J^d, J^{ad}) = \hat{H}(\hat{S}_a, \tau_d\hat{S}_d, J^a, J^d, -J^{ad}) = \hat{H}(\tau_a\hat{S}_a, \hat{S}_d, J^a, J^d, -J^{ad}). \tag{3}$$

At the level of the MF approximation the relations (3) become a property of the Hamilton function of the system and thus they determine the symmetry of the magnetic phase diagrams of YIG in the space of the superexchange coupling parameters J^a, J^d and J^{ad}. In particular, if the point $p = (J^a, J^d, J^{ad})$ corresponds to a ferromagnetic phase then, in general, for the

point $p' = (J^a, J^d, -J^{ad})$ a certain ferrimagnetic phase is stable. The energies E_p and $E_{p'}$ of the respective phases are equal to each other. However, it does not mean that magnetic excitation energies will be equal, because they depend on sign of J^{ad}.

It can be easily shown that the group of transformations $\mathcal{G}$ can be extended to the Hamiltonian symmetry group $\{\tilde{e}, \tilde{\tau}_a, \tilde{\tau}_d, \tilde{\tau}\}$, where $\tilde{e} = e \times 1$, $\tilde{\tau}_a = \tau_a \times -1$, $\tilde{\tau}_d = \tau_d \times -1$, $\tilde{\tau} = \tau \times 1$ and ± 1 are coefficients accompanying J^{ad}. That is why we shall use the same symbol for the group $\mathcal{G}$ and its extension. We should bear in mind that this group is essentially different from O_h^{10}, i.e. it acts in an entirely different space.

3. A method for the determination of the ground state

3.1. Valleys of the Hamilton function and the ground state

In order to obtain a phase diagram, a quasi-classical approximation is applied to the Hamiltonian (1). All the spin operators $\hat{s}_i$ of (1) are substituted by the classical three-dimensional vectors $s\boldsymbol{s}_i$ where $\boldsymbol{s}_i$ are normalized to unity and $s = \frac{5}{2}$.

Within the framework of this approximation the operator $\hat{H}$ turns into a classical Hamilton function as follows:

$$\mathcal{H}/s^2 = -\frac{1}{2}\sum_{i \neq j} J_{ij}^a \boldsymbol{s}_i \boldsymbol{s}_j - \frac{1}{2}\sum_{k \neq l} J_{kl}^d \boldsymbol{s}_k \boldsymbol{s}_l - \sum_{i,k} J_{ik}^{ad} \boldsymbol{s}_i \boldsymbol{s}_k \tag{4}$$

where $\boldsymbol{s}_i \boldsymbol{s}_j$ is a scalar product of the unit vectors $\boldsymbol{s}_i$ and $\boldsymbol{s}_j$. The configuration space $\mathcal{M}$ of the function $\mathcal{H}$ is an N-fold cartesian product of the two-dimensional spheres $\mathbf{S}^2$: $\mathcal{M} = \prod_{i=1}^{N} \mathbf{S}^2$, where N is the number of spins in the system.

It can be easily shown that the replacement of the determination of the quantum ground-state problem with its quasi-classical equivalent consists in finding the latter in the set of trial functions which are the coherent states [11].

The symmetry of the function (4) like that of the Hamiltonian (1) is determined by the three following groups: $O(3)$, O_h^{10} and $\mathcal{G}$.

Having rewritten the vectors $\boldsymbol{s}_i$ in spherical coordinates, $\boldsymbol{s}_i = (\sin\vartheta_i \cos\varphi_i, \sin\vartheta_i \sin\varphi_i, \cos\vartheta_i)$, we obtain the following set of stationary equations for the ground state:

$$\frac{\partial \mathcal{H}}{\partial \varphi_i} = 0 \qquad \frac{\partial \mathcal{H}}{\partial \vartheta_i} = 0 \qquad i \in a, d.$$

In order to interpret different solutions of these equations we resort to an analysis based on the symmetry. In particular, two solutions $\mathcal{S} = (\boldsymbol{s}_i)$ and $\mathcal{S}' = (\boldsymbol{s}_j')$ are considered as being different from each other if one cannot be transformed into the other under any rotation g of the group $O(3)$. This natural definition leads us to the conclusion that the whole orbit

$$V = \{(\boldsymbol{s}_i') : (\boldsymbol{s}_i') = (g\boldsymbol{s}_i),\ g \in O(3)\} \tag{5}$$

should be considered as one solution of the stationary equations. Of course, the Hamiltonian function $\mathcal{H}$ is constant on the orbits. If any point of the orbit V corresponds to a local minimum of the function $\mathcal{H}$, then the whole set V is called a valley in the state space $\mathcal{M}$. This notion is borrowed from the theory of spin glasses [1, 2] and has turned out also to be useful in the case of the function (4).

If the function $\mathcal{H}$ has at least two different valleys V_1 and V_2 corresponding to the global minimum of energy, then we say that the ground energy level of the system is non-trivially degenerate. If, in addition, these valleys are separated from one another by non-vanishing energy barriers, then frustrations are bound to occur in the system [1, 2].

In this paper, the ground state will be defined as the state of lowest energy in which the period of the spin correlations is identical with that of the crystal lattice. This assumption enables us to reduce the number of stationary equations to 40 pairs for an elementary cell with periodic boundary conditions. The stationary equations are non-linear and complicated. Therefore we resort to another method of determining a ground state of the system. We have adapted the so-called relaxation method which hereto had mostly been used for disordered systems. The relaxation method, was proposed for the first the time in [1] and was later discussed in great detail in [2].

3.2. The relaxation method

Obviously spins tend to take orientations parallel to local molecular magnetic fields. This can be neatly expressed by the relaxation procedure, where we have the following equations for determining the equilibrium spin configurations:

$$s_i = F_i(\mathcal{S}) \qquad i = 1, \ldots, N \tag{6}$$

where

$$F_i(\mathcal{S}) = \frac{\sum_j J_{ij} s_j}{\| \sum_j J_{ij} s_j \|} \qquad \mathcal{S} = (s_1, \ldots, s_N) \tag{7}$$

and $\| \sum_j J_{ij} s_j \|$ denotes the norm. The relaxation procedure for

$$s_i^{n+1} = F_i(\mathcal{S}^n) \tag{8}$$

is repeated as many times as needed to satisfy

$$\frac{1}{N} \sum_i \| s_i^{n+1} - s_i^n \| \leqslant \varepsilon \tag{9}$$

where ε denotes the assumed accuracy. In the majority of cases it is sufficient to take $\varepsilon = 10^{-8}$ [2]. The solutions obtained within the framework of this method are only local minima (metastable configurations) of the Hamiltonian function $\mathcal{H}$.

It is easily seen that the equilibrium positions of the spins are fixed points of the set of functions $(F_1, \ldots, F_N)$. Equations (8), in principle, are not simpler than the stationary equations, but the former's iterations are convergent.

Another important property of (8) is their $O(3)$ invariance, i.e.

$$g s_i = F_i(g\mathcal{S}) \qquad i = 1, \ldots, N \qquad g \in O(3). \tag{10}$$

These relations actually mean that the fixed points of (8) form the whole valleys of the function $\mathcal{H}$ and that all the points of a given valley V are equally attainable in the iteration process. This homogeneity of all the points of the valleys of the Hamiltonian function $\mathcal{H}$ with respect to the iteration of (8), turns out to be very useful in the Monte Carlo numerical

calculations of certain integrals which characterize a degree of inhomogeneity of the spin correlation functions (see the next section).

In order to obtain a phase diagram of YIG we apply the relaxation procedure to the spins of an elementary unit cell. Consequently, in (6) N is equal to $N_a + N_d = 40$. The periodic boundary conditions are imposed on the superexchange couplings J_{ij}^a, J_{ij}^d and J_{ij}^{ad}. To achieve an accuracy of $\varepsilon = 10^{-8}$ it is usually sufficient to perform several tens of reorientations of the spins with the aid of (8). If the spins s_i have a configuration corresponding to the global minimum of the function $\mathcal{H}$, then it can easily be tested whether they are, for instance, collinear. It is also easy to determine the resultant magnetization M of the elementary cell:

$$M = M_a + M_d \tag{11}$$

where M_a and M_d are the resultant magnetization of the sites (a) and (d) of the elementary unit cell, respectively, for example $M_a = \sum_{i \in a} s_i$, where the summation runs over all the 16 (a) sites.

By studying the magnetization, collinearity of the spins, degeneracy of a ground state and so on for different sets of the superexchange parameters J^a, J^d and J^{ad}, we can determine a phase diagram of the system at $T = 0\,\mathrm{K}$.

It is worth noting here that the phase space of the system is actually two-dimensional, since by a simple rescaling we can get the ratios $J^a/|J^{ad}|$ and $J^d/|J^{ad}|$ with $J^{ad} \neq 0$ as parameters of the function $\mathcal{H}$; $J^{ad} = 0$ corresponds to two mutually independent spin subsystems which appear in the crystal sublattices (a) and (d).

3.3. The concept of information entropy and density of the spin correlation functions at T = 0 K

Let us assume now that a state is essentially degenerate if its energy E is a local minimum of the Hamilton function $\mathcal{H}$. This means that there exist a number of different valleys $V_1, V_2, V_3, \ldots$ corresponding to the state. One can then pose the question: does a certain spin correlation function f take the same values for all these valleys? Of course, the question makes sense only for correlation functions that have the same gauge symmetry as that of the Hamilton function $\mathcal{H}$, i.e. for the correlation functions for which $f(g\mathcal{S}) = f(\mathcal{S})$ for all rotations g of the group $O(3)$. One must realize, however, that the number of valleys $V_1, V_2, V_3, \ldots$ with the same energy can be quite large, particularly in a frustrated system. Then, instead of giving a series of numbers $f(V_1), f(V_2), f(V_3), \ldots$, it is easier to specify how many different valleys can be located in a given range $[x, x + \Delta x]$, where $x = f(\mathcal{S})$. In other words, we define the density $\rho_f(x, E)$ of the correlation function $x = f(\mathcal{S})$ in the space of all the valleys with the same energy E.

In the case of a global minimum (with energy E_0) of the Hamilton function $\mathcal{H}$ the following method can be used to determine the density $\rho_f(x, E_0)$. We heat our system to a high temperature and then follow how the $O(3)$-invariant correlation function f changes as the temperature drops back to zero. It is clear that the probability of finding at $T = 0\,\mathrm{K}$ a value of the function f in the small range $[x, x + \Delta x]$ is equal to $\rho_f(x, E_0)\Delta x$.

The density $\rho_f(x, E_0)$ has two important properties. First, it determines the distribution of the function f on the valleys $V_1, V_2, V_3, \ldots$. Second, it determines the frequency at which the system falls into different valleys while the temperature decreases. The second of these properties strongly depends upon the form that the Hamilton function $\mathcal{H}$ takes in the vicinity of the valleys with energy E_0; for instance, in the case of a frustrated system

the frequency at which the system falls into different valleys is strongly dependent upon the height and form of barriers separating the valleys from one another.

The mathematical expression of high temperatures is a random orientation of the spins. We choose at random, in the configuration space $\mathcal{M}$ of the Hamilton function $\mathcal{H}$, a certain number of points $\mathcal{S}_1, \ldots, \mathcal{S}_L$, where

$$\mathcal{S}_\alpha = (s_{1,\alpha}, \ldots s_{N,\alpha}) \qquad \alpha = 1, \ldots, L. \tag{12}$$

Let these points evenly cover the manifold $\mathcal{M}$. Simultaneously, within the framework of the relaxational procedure, a certain ground state $\mathcal{S}_\alpha^0 = (s_{l,\alpha}^0)$ can be obtained from every point $\mathcal{S}_\alpha$, at which point the value f_α^0 of the function f is found to be equal to $f_\alpha^0 = f((s_{l,\alpha}^0))$. The measure, which has been already mentioned, is defined by the density histogram:

$$\rho_f(x_l, E_0) = \frac{n_l}{L\Delta x} \tag{13}$$

where n_l is the number of values f_α^0 that fulfill the condition

$$x_l \leqslant f_\alpha^0 \leqslant x_l + \Delta x \tag{14}$$

where Δx is very small. Moreover, it is assumed that $x_l = l\Delta x$, $l = 0, \pm 1, \pm 2, \ldots$. In order to provide an even distribution of the points $\mathcal{S}_1, \ldots, \mathcal{S}_L \in \mathcal{M}$ we can determine their positions by a random number generator. Since our configuration space is an $N_a + N_d = N$-fold cartesian product of the two-dimensional unit spheres, a large number (at least 10^4) of points l is necessary for the calculation of the density ρ_f.

A simple but interesting example of the $O(3)$-invariant correlation functions is given by

$$f_{nm}(\mathcal{S}) = \cos^{-1}(s_n s_m) \tag{15}$$

where $\mathcal{S} = (s_1, \ldots, s_n, \ldots, s_m, \ldots)$. Another example of a gauge-invariant spin correlation is given by a function which is proportional to the magnetic susceptibility of the system:

$$\kappa = \kappa^{xx} + \kappa^{yy} + \kappa^{zz} = \frac{1}{N} \sum_{i,j} s_i s_j. \tag{16}$$

For every such function an appropriate density $\rho_f(x, E_0)$ can be found. If the latter is characterized by one sharp peak then, in spite of the non-trivial degeneracy of the ground state, the correlation function f will not behave randomly with lowering temperature.

A measure of randomness for a given function is its information entropy, defined as follows:

$$H_f = -\int \mathrm{d}x\, \rho_f(x, E_0) \log\bigl(\rho_f(x, E_0)\bigr). \tag{17}$$

The upper limit of the information entropy H_{nm} corresponding to the function (15) can be estimated by the information entropy of the uniform distribution. The angle between two spins takes values in the range $(0°, 180°)$ where the uniform distribution has a maximum value equal to $1/180$ and thus $H_{nm} \leqslant \log(180) \cong 5.19295$.

If all mutually independent correlation functions of the system have their information entropy H_{nm} comparable with log(180), then we say that such a system resembles an ideal spin glass. In other cases, one can speak only of a semi-spin glass. A semi-spin glass behaviour means that only certain parts of the whole system have correlation functions with their densities spread out on the domain field. One can also imagine a system consisting of parts inside which there is no spin glass, but the inter-subsystem correlation functions behave randomly.

This definition of a spin glass is wider than that based on the concept of frustrations. According to our definition, we can also classify as spin glasses such systems whose ground energy level displays a non-trivial degeneracy but whose different valleys $V_1, V_2, V_3, \ldots$ are not necessarily separated from one another by the energy barriers. In such exotic spin glasses, in the space of the valleys $V_1, V_2, V_3, \ldots$ there appears an additional symmetry which results from the specific geometry of the system and is connected with its space group, the range of the superexchange interactions, and so on. As can be easily seen, the exotic spin glasses are usually ergodic whereas the spin glasses with frustrations, in general, are not.

4. Results

4.1. Phase diagrams of the ground states

For $J^{ad} = 0$ the system can be considered as one consisting of two mutually independent spin subsystems (a) and (d) with periodic boundary conditions. Resorting to the relaxation method one obtains the following results. For $J^a > 0$ ($J^d > 0$) the ground state of the sublattice (a) (or (d)) is purely ferromagnetic, whereas for $J^a < 0$ ($J^d < 0$) a purely antiferromagnetic ground state is obtained for the (a) (or (d)) sublattice.

For $J^{ad} \neq 0$ the ground state of the system depends upon the sign of the inter-sublattice superexchange integral, J^{ad} and the ratio of the inter- to intra-sublattice integral, i.e. $J^a/|J^{ad}|$ and $J^d/|J^{ad}|$. Since the Hamiltonian (4) is invariant under the operators of the inversion group $\mathcal{G}$, stable phases of the ground energy level diagrams for $J^{ad} < 0$ (see figure 1(a)) and $J^{ad} > 0$ (see figure 1(b)) are strongly mutually dependent.

In both phase diagrams of figure 1(a) and 1(b) there appear AF-I and AF-II phases with the resultant magnetic moments M_a and M_d of the sublattice (a) and (d) equal to zero. The AF-I phase is not a frustrated semi-spin-glass. Different valleys $V_1, V_2, V_3, \ldots$ corresponding to its ground energy level are separated from one another by no energy barriers. On the other hand, the AF-II phase is a frustrated semi-spin-glass, i.e. the valleys of its ground energy level are separated from one another by energy barriers. It seems that the degeneracy of the phases AF-I and AF-II results from the special garnet geometry described by the space group O_h^{10}.

The AF-II phase (the 'boomerang' region in figures 1(a) and 1(b)) is characterized by a 'spatial' distribution of the magnetic moments either in the sublattice (a) or (d), i.e. in at least one of these sublattices there exist three linearly independent spins. In the spin-glass phase AF-I, each sublattice displays a pure antiferromagnetic ordering but the angle between the magnetic moments of the sublattices can take any value in the range 0°–180°. We now discuss the differences between the phase diagrams of figures 1(a) and (b). Figure 1(a), shows three non-degenerate regions: Ferri-I, Ferri-II and Ferri-III.

In the phase Ferri-I each sublattice is a collinear ferromagnet but the sublattice resultant magnetizations are opposite to each other. Since the sublattices have different numbers of

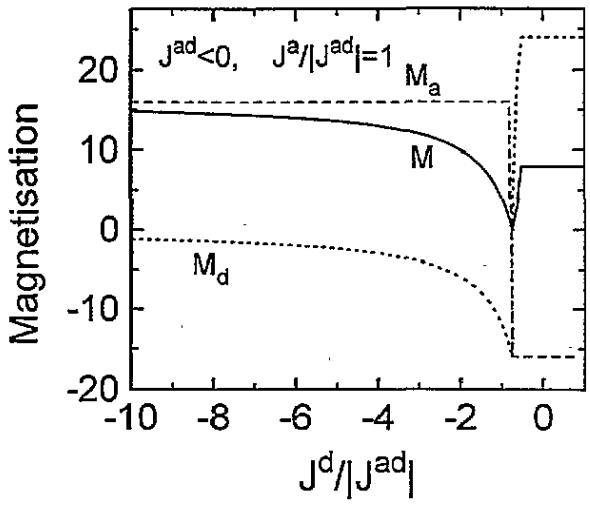

Figure 2. The resultant magnetization (full curve) and magnetizations of the sublattices (a) (broken curve) and (d) (dotted curve) against the ratio $J^d/|J^{ad}|$ for $J^{ad} < 0$ and $J^a/|J^{ad}| = 1$.

spins, the total resultant magnetization is not equal to zero and therefore, the phase Ferri-I can be considered either as a ferrimagnet or an uncompensated antiferromagnet.

In the Ferri-II phase, magnetic moments of both sublattices are parallel to a certain plane, π_d. However, the sublattice (a) is a collinear ferromagnet, whereas the spins of the sublattice (d) form different angles with one another. The resultant magnetization of the sublattice (d) is opposite to that of the sublattice (a). Since with increasing J^d the length of the vector M_d also increases, there occurs in figure 1(a) the broken line on which the resultant moments M_a and M_d compensate each other, and the total resultant moment M is zero. The line separating the phases AF-II and Ferri-II from each other, is a line of non-continuous changes of the magnetization.

The phase Ferri-III is analogous to the phase Ferri-II but with the roles of the sublattices inverted. Again, magnetic moments of the sublattices (a) and (d) are parallel to a certain plane π_a. This time, however, spins of the sublattice (d) are ordered ferromagnetically along one direction whereas spins of the sublattice (a) form different angles with one another. The resultant magnetic moment M_d is opposite to the resultant magnetization M_a. The number of spins in the sublattice (d) is bigger than that in the sublattice (a) and, consequently, no compensation line appears in this region and there is no spin-flop phase. On the broken line, separating the phases Ferri-I and Ferri-II from each other, the resultant magnetization M is a continuous function of the parameters J^a and J^d.

In figure 1(b) ($J^{ad} > 0$) there appear three regions called Ferro-I, Ferro-II and Ferro-III. These phases are non-degenerate and can be obtained from the analogous phases Ferri-I, Ferri-II and Ferri-III under the operations of the inversion group $\mathcal{G}$, i.e.

$$\begin{aligned} &\text{Ferro-I} = \tau_a(\text{Ferri-I}) = \tau_d(\text{Ferri-I}) \\ &\text{Ferro-II} = \tau_a(\text{Ferri-II}) = \tau_d(\text{Ferri-II}) \\ &\text{Ferro-III} = \tau_a(\text{Ferri-III}) = \tau_d(\text{Ferri-III}). \end{aligned} \tag{18}$$

The first of these equations means that both sublattices (a) and (d) are ferromagnetically ordered and their effective magnetizations M_a and M_d are parallel to each other.

The second equation of (18) suggests that magnetic moments of both sublattices are parallel to the same plane π_d. Magnetic moments of the sublattice (a) are ordered ferromagnetically, whereas those of the sublattice (d) make different angles to one other. The resultant magnetization M_d is directed along the magnetization M_a. The third equation of (18) should be understood in the same way.

In the regions Ferri-I, Ferro-I, AF-I and AF-II the magnetization M is constant and is equal to 8, 40, 0, 0 respectively. In the regions Ferri-II (Ferro-II) and Ferri-III (Ferro-III) the magnetization is constant along the lines parallel to the axes $J^a/|J^{ad}|$, $J^d/|J^{ad}|$ respectively. The diagrams of the magnetization perpendicularly to the coordination axes are given in figure 2. This figure, presenting a transition through the spin-flop phase, is particularly noteworthy. The mutual characteristic of all the diagrams of the magnetizations is the latter's asymptotic vanishing for large negative values of $J^d/|J^{ad}|$ or $J^a/|J^{ad}|$ in the sublattice whose spins are not parallel to one another.

All these properties of the magnetic ground state of yttrium iron garnets, and in particular the occurrence of spin-glass phases, result from the complex geometry of YIG where two sublattices of cations interpenetrate each other, forming a non-equivalent nearest-neighbour vicinity around sites of either sublattice. For instance, in the AF-I phase a molecular field acting on spins of the sublattice (a), and produced by the spins of the sublattice (d), takes the following form:

$$h_l = \sum_{j \in d} J_{lj}^{ad} s_j \qquad l \in a \tag{19}$$

and appears to be equal to zero as the antiferromagnetically ordered spins s_j compensate each another. It is also true about the molecular field coming from the sublattice (d), acting on a spin of the sublattice (a). So both sublattices are mutually independent despite J_{ad} being non-zero.

4.2. Densities of the correlation function in the spin-glass phases

In order to obtain more precise characteristics of the spin-glass phases in AF-I and AF-II regions let us study the question of the spin correlation functions in more detail.

The following functions of spin correlations in the sublattice (a) can be defined:

$$f_{\mathrm{NN}}^{aa} = \cos^{-1}(s_i s_j) \qquad f_{\mathrm{NNN}}^{aa} = \cos^{-1}(s_k s_l) \tag{20}$$

where $i, j, k, l \in a$ and the indexes (NN) and (NNN) denote nearest (i, j) and next nearest (k, l) neighbours, respectively.

The spin correlation functions in the sublattice (d) f_{NN}^{dd} and f_{NNN}^{dd} are defined in the same way as given by (20) for the sublattice (a). The inter-sublattice correlation are described by the following functions:

$$f_{\mathrm{NN}}^{ad} = \cos^{-1}(s_i s_j) \qquad f_{\mathrm{NNN}}^{ad} = \cos^{-1}(s_k s_l) \tag{21}$$

where $i, k \in a$ and $j, l \in d$.

In the ground state these correlation functions determine the densities according to the scheme given in section 3, for instance

$$\rho_{\mathrm{NN}}^{aa}(\alpha) = \rho_{f_{\mathrm{NN}}^{aa}}(\alpha, E_0) \tag{22}$$

where $\alpha \in (0°, 180°)$.

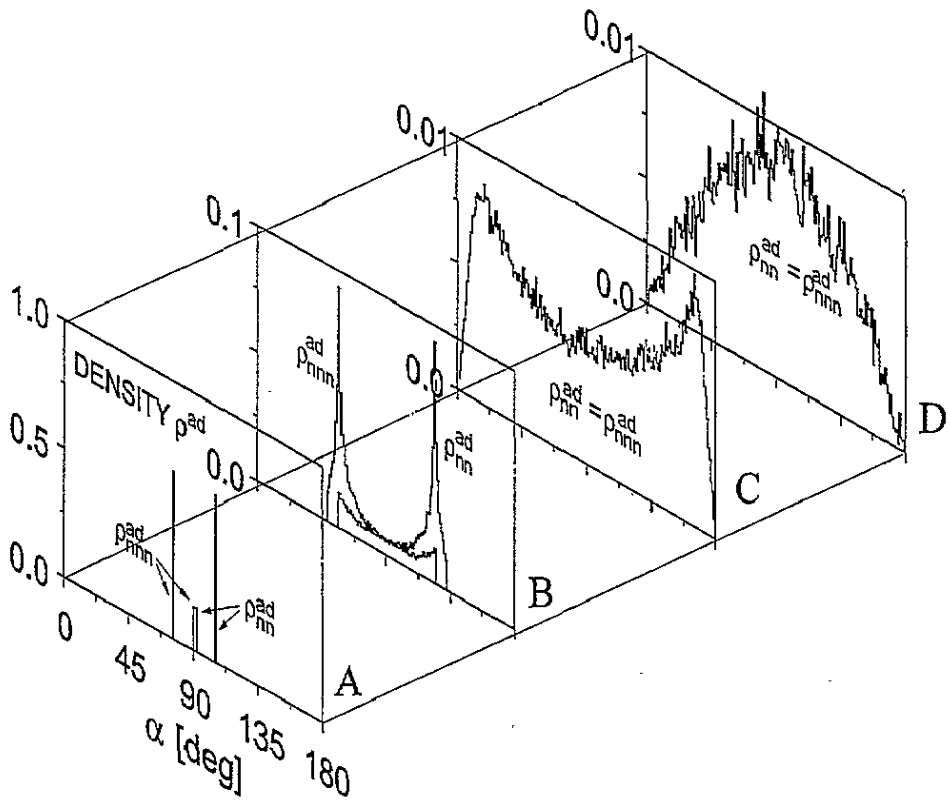

Figure 3. The density spin correlation function ρ^{ad} for different points A, B, C, D from the phase diagram for $J^{ad} < 0$ (see figure 1(*a*)) for nearest neighbours (NN) and next-nearest neighbours (NNN) (*a*-*d*). The points A = $(-0.1, -2)$ and B = $(-0.9, -0.2)$ both lie in the AF-II phase. The points C = $(-0.6, -0.6)$ and D = $(-3, -3)$ both lie in the AF-I phase. The information entropies H_f for these points are respectively $H^{ad}_{A} = 1.0984$, $H^{ad}_{B} = 3.9911$, $H^{ad}_{C} = 5.1438$, $H^{ad}_{D} = 5.0466$. These entropies are the same for the nearest and next-nearest neighbours.

The histograms of these densities for certain values of the parameters $J^d/|J^{ad}|$ and $J^a/|J^{ad}|$ are given in figures 3 and 4. The figure captions give the values of the information entropy $H^{aa}_{NN}, \ldots, H^{ad}_{NN}$ and H^{ad}_{NNN}. The calculations were carried out choosing at random the number L of 10^4 points assuming the homogeneous distribution in the configuration space $\mathcal{M}$ of a single elementary cell. The range of permitted angles α is divided into 180 equal parts, so that all the correlation figures present the densities of the range $\Delta\alpha = 1°$.

The diagrams grow smoother with increasing number L. This is typical of the Monte Carlo method.

Figures 3 and 4 show clearly that the phases AF-I and AF-II differ significantly from each other with respect to their spin correlations. This is seen in particular from the diagrams of the density $\rho^{ad}_{NN}(\alpha)$ and $\rho^{ad}_{NNN}(\alpha)$.

In the phase AF-I, the densities $\rho^{aa}_{NN}(\alpha)$ and $\rho^{aa}_{NNN}(\alpha)$ (or $\rho^{dd}_{NN}(\alpha)$, $\rho^{dd}_{NNN}(\alpha)$) display well localized peaks for $\alpha = 0°$ and $\alpha = 180°$, which correspond to the purely antiferromagnetic correlations in the sublattice (*a*) (or (*d*)). The inter-sublattice densities $\rho^{ad}_{NN}(\alpha)$ and $\rho^{ad}_{NNN}(\alpha)$ take non-zero values for the whole range of the angles, i.e. from 0° to 180°. This clearly indicates a spin-glass behaviour of the spins.

The behaviour of the spin correlations in the phase AF-II is strange. All the densities ρ take non-zero values only for certain regions or even single values from the range 0°, 180°. This enables us to consider AF-II as a semi-spin-glass phase.

Apart from ρ_{NN} and ρ_{NNN}, the density $\rho_\kappa(x, E_0)$ where $x \in (0, 1)$, of the correlation function κ given by (16) has also been calculated. In both phases AF-I and AF-II, $\rho_\kappa(x, E_0)$ has the same form with the peak localized at $x = 0$. This shows clearly that the function κ in these phases is not random and, moreover, that its behaviour is analogous to that for a paramagnet at infinite temperature, or an antiferromagnet at $T = 0$ K.

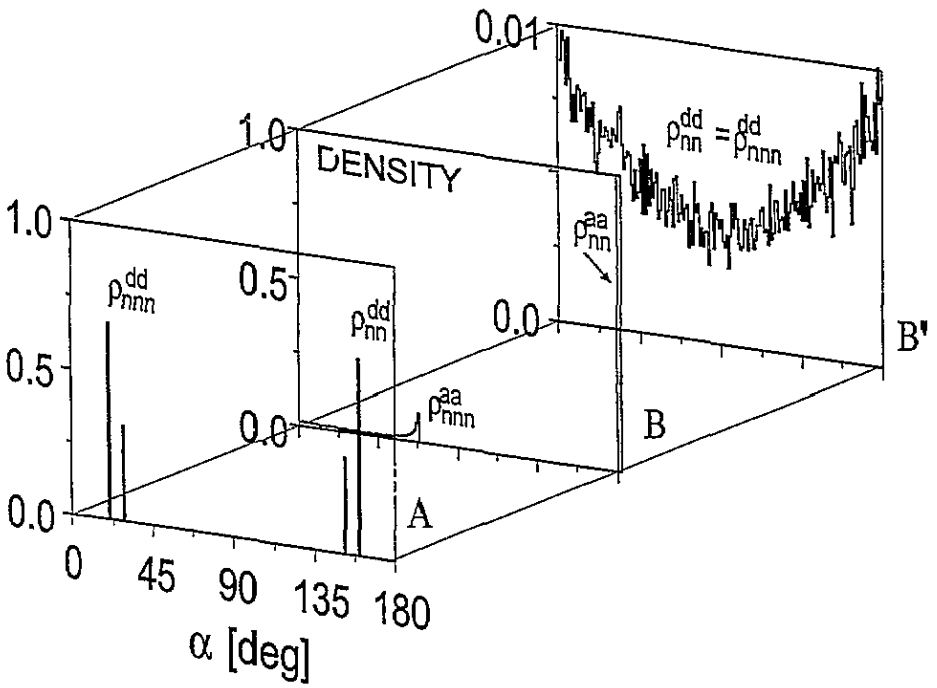

Figure 4. The density spin correlation function ρ^{dd} and ρ^{aa} for different points A, B, B' from the phase diagram for $J^{ad} < 0$ (see figure 1a) for nearest neighbours (NN) and next-nearest neighbours (NNN) (d-d) and (a-a). The positions of the points A and B (B' = B) are the same as on the figure 3. The information entropies H_f for these points are respectively $H^{dd}_A = 0.6334$, $H^{aa}_{B,NNN} = 3.9887$, $H^{aa}_{B,NN} = 0$, $H^{dd}_{B'} = 5.1497$.

5. Conclusions

The dimension of the phase diagram in our model of YIG is reduced to two by choosing the ratios $J^a/|J^{ad}|$ and $J^d/|J^{ad}|$ as parameters. For both cases of $J^{ad} < 0$ and $J^{ad} > 0$ the magnetic ground-state phase diagram is divided into five different regions from which three are of the non-degenerate ferromagnetic (if $J^{ad} > 0$) or ferrimagnetic (for $J^{ad} < 0$) type, whereas the two remaining ones of the antiferromagnetic type display a non-trivial high degeneracy.

This degeneracy is caused by the frustrations. That is why these phases are of semi-spin-glass type. The source of frustrations, in turn, is the particular geometry of sub-lattices (a) and (d) which are occupied by magnetic ions Fe^{3+}.

It seems that the best way of describing them, which can be applied particularly to the highly degenerate phases, should be based on the idea of spin-correlation density and information entropy. In particular, very interesting results are obtained in the 'boomerang' AF-II phase which displays strong inhomogeneity with respect to the spin-correlation density according to values of the superexchange parameters (see figures 3 and 4).

The ferrimagnetic point G of the phase diagram, corresponding to real $Y_3Fe_5O_{12}$ yttrium iron garnet is in the close vicinity of the AF-II, Ferri-II and Ferri-III phases (see figure 1(a)). This might be the cause of the high sensitivity of YIG to doping. The location of the point G in figure 1(a) is obtained from experimentally fitted values of the superexchange integrals J^a, J^d and J^{ad} [3] in the fourth-order of perturbation calculations of the magnetization. However, we should realize that for years there has been no consensus on the location of the point G. This is caused by difficulties arising from (i) the inaccuracy of the estimation of exchange integrals in effective field models [13], and (ii) loss of information of real sources of resultant magnetization and degrees of contributions from the sublattices [14, 15].

However, if we take the most well known estimations of G point locations, as quoted by Strentzwik and Anderson [3] in their table 1, and mark them on the graph in figure 1(a) we shall find that the majority of the estimations fall in the zone that is entirely contained in the Ferri-I phase and delimited by the graph axes passing through the origin and the lines separating phases Ferri-II, Ferri-III and AF-II. For example, the estimations of Wojtowicz [16] fall close to the origin, while the ones obtained by Harris [17] are halfway between that of Wojtowicz and that of Strentzwik and Anderson.

The location of the G point can explain the anomalous low-temperature magnetic properties of YIG doped with uncompensated ions Ca^{2+}. In particular, the low-temperature decrease of its saturation magnetization [4]. Because of their size the calcium Ca^{2+} ions occupy sites in the sublattice (c), thus the YIG properties cannot be explained as the direct result of dilution of ions entering into (a) and/or (d) sublattices.

We think that the location of the $G(x)$ point on the diagram (see figure 1(a)) of the doped garnet $(Y_{3-x}Ca_x)Fe_5O_{12}$ can be calculated [6] within the framework of a previously introduced model [9, 10]—an adaptation of the usual periodic Anderson model for the narrow-band (3d) and wide-band (2p) band electrons with the (p-d) hybridization term.

The location changes mechanism of the point $G(x)$, expressed as a function of x, is associated with the modification of super-exchange integrals calculated at the fourth-order terms of perturbation calculus relative to hybridization term (see also [9, 10]).

The relaxation method, which has been used throughout the paper, can also be applied to a number of different magnetic systems particularly those with complex magnetic unit cells, long-distant magnetic interactions, and so on.

This method was recently applied to a description of the magnetic ground state of the fullerene family C_N. As it turns out, this state happens to be frustrated. We found the notion of correlation density function very useful here too. It enabled us to trace regularities in changes of the ground state with changing number of carbon atoms [11].

Acknowledgments

We wish to thank Professor P E Wigen and his group for sharing their interesting experimental results which have contributed to our theoretical analysis. Thank are also due

to Dr L Pust and Dr A Maziewski for many fruitful discussions about their experiments in garnets. We are very grateful to Professor D L Huber for his inspiring discussions concerning complex spin systems. The research was supported by the Committee for Scientific Research under the grant no. 3 P408 001 04.

References

[1] Walker L R and Walstedt R E 1977 *Phys. Rev. Lett.* **38** 514; 1980 *Phys. Rev.* B **22** 3816
[2] Henley Ch L 1984 *Ann. Phys.* **156** 324, 368
[3] Strentzwilk D F and Anderson E E 1968 *Phys. Rev.* **175** 654
[4] Wigen P E and Pardavi-Horvath M 1987 *Physics of Magnetic Materials* ed. W Gorzkowski, H K Lachowicz and H Szymczak (Singapore: World Scientific)
[5] Brückel Th, Prandl W and Convert P 1987 *J. Phys. C: Solid State Phys.* **20** 2565
[6] Lehmann-Szweykowska A, Wojciechowski R and Koper A 1994 in preparation
[7] Lehmann-Szweykowska A, Koper A, Wojciechowski R and Tomalak T 1992 *J. Magn. Magn. Mat.* **104–7** 477
[8] Koper A, Lehmann-Szweykowska A and Wojciechowski R 1992 *Physica* B **180–1** 133
[9] Lehmann-Szweykowska A, Wojciechowski R, Pust L, Wigen P E and Batra S 1991 *Phys. Rev.* B **43** 3500
[10] Lehmann-Szweykowska A, Wojciechowski R, Pust L, Wigen P E and Batra S 1991 *J. Appl. Phys.* **69** 4648
[11] Koper A, Stankowski J and Thomas M 1994 *Acta Phys. Pol.* A **25** 351
[12] Wadas R S 1974 *Magnetism in Spinels, Garnets and Perovskites* (Warsaw: PWN) ch 5
[13] Smart J S 1956 *Phys. Rev.* **101** 585
[14] Prince E 1964 *J. Physique* **25** 503
[15] Tinsley C J 1987 *Phil. Mag.* B **56** 351
[16] Wojtowicz P J 1965 *Proc. Int. Conf. on Magnetism, Nottingham, 1964* (London: The Physical Society) p 11
[17] Harris A B 1963 *Phys. Rev.* **132** 2398